

REPORT DOCUMENTATION PAGE

Form Approved
OMB No. 0704-0188

Public reporting burden for this collection of information is estimated to average 1 hour per response, including the time for reviewing instructions, searching existing data sources, gathering and maintaining the data needed, and completing and reviewing this collection of information. Send comments regarding this burden estimate or any other aspect of this collection of information, including suggestions for reducing this burden to Department of Defense, Washington Headquarters Services, Directorate for Information Operations and Reports (0704-0188), 1215 Jefferson Davis Highway, Suite 1204, Arlington, VA 22202-4302. Respondents should be aware that notwithstanding any other provision of law, no person shall be subject to any penalty for failing to comply with a collection of information if it does not display a currently valid OMB control number. **PLEASE DO NOT RETURN YOUR FORM TO THE ABOVE ADDRESS.**

1. REPORT DATE (DD-MM-YYYY)		2. REPORT TYPE	3. DATES COVERED (From - To)		
4. TITLE AND SUBTITLE			5a. CONTRACT NUMBER		
			5b. GRANT NUMBER		
			5c. PROGRAM ELEMENT NUMBER		
6. AUTHOR(S)			5d. PROJECT NUMBER		
			5e. TASK NUMBER		
			5f. WORK UNIT NUMBER		
7. PERFORMING ORGANIZATION NAME(S) AND ADDRESS(ES)			8. PERFORMING ORGANIZATION REPORT NUMBER		
9. SPONSORING / MONITORING AGENCY NAME(S) AND ADDRESS(ES)			10. SPONSOR/MONITOR'S ACRONYM(S)		
			11. SPONSOR/MONITOR'S REPORT NUMBER(S)		
12. DISTRIBUTION / AVAILABILITY STATEMENT					
13. SUPPLEMENTARY NOTES					
14. ABSTRACT					
15. SUBJECT TERMS					
16. SECURITY CLASSIFICATION OF:			17. LIMITATION OF ABSTRACT	18. NUMBER OF PAGES	19a. NAME OF RESPONSIBLE PERSON
a. REPORT	b. ABSTRACT	c. THIS PAGE			19b. TELEPHONE NUMBER (include area code)

Novel Protein Folding Pathways for Protein Salvage and Recycling

Frank Robb, PI. University of Maryland
Igor Lednev, CoPI University of New York at Albany

Summary

Proteostasis is the term used to describe the combined mechanisms by which cells maintain their peptides and proteins in soluble and functional status. This is accomplished through the actions of multiple chaperones that carry out cooperative protein folding and unfolding reactions. Archaea are primitive microorganisms placed by most taxonomic criteria at the base of the Tree of Life. The Archaea have many molecular properties that are found universally in modern lineages of both Bacteria and Archaea, and many species are specialized for survival and growth in extreme conditions, including at or above the normal boiling point of water. These hyperthermophilic archaea have greatly reduced genomes and proteomes compared to many mesophiles, and proteostasis in Archaea is considerably simplified compared with either eukarya or bacteria. In hyperthermophiles, the chaperonin (Cpn60) is the only ATP dependent protein folding complex. It is a 1 mDa molecular machine formed by two stacked rings of subunits; each ring forms a chamber that opens and closes in an alternate cycle, like a reciprocal 2-stroke internal combustion motor.

We hypothesized that hyperthermophilic Archaea carry out both protein folding and unfolding tasks using a single basic pathway in which the Cpn60 is central.

Our specific aims were

1. To determine the mechanistic basis for switching the Cpn from folding to unfolding in order to unfold or modify nanoscale complexes efficiently.
2. To determine the regulation of cellular responses to heat shock and unfolded proteins in genetically enabled hyperthermophiles.

We proposed a new method of molecular analysis of the chaperonin in which Hsp60 oligomers are mutated to operate efficiently at human physiological temperatures. By examining the unfolding action we will duplicate the stress responses that enable the hyperthermophiles' chaperones to disperse and recycle denatured proteins. The folding alterations of the target proteins was assessed with Deep UV Raman Spectroscopy and Circular Dichroism spectroscopy, and visualized with Scanning Electron Microscopy and Atomic Force Microscopy .

In order to study protein folding in vivo, we reconstructed archaeal folding systems in *E. coli* and also use a new genetic system allowing recombinant expression of heterologous proteins, overexpression of native proteins and knockouts in a versatile hyperthermophilic archaeon with a very broad temperature range.

Our recent work suggests that fibrillar proteins may trigger the unfolding

response of the archaeal Cpn60 to enable the dispersion and solubilization of aggregated proteins(1, 2). Our results suggest that there are periodic entry points on the surface of nanoscale fibrils.

Experimental Results

1. Chaperonin cloning, expression and rational mutation studies.

The chaperones from hyperthermophiles must be extraordinarily stable in order to sustain the repair and salvage functions that these organisms must exert to remain viable at or above 100C. Fig 1 shows the stability and activity of the Group 1 Cpn60 from *Pyrococcus furiosus* in Guanidine Hydrochloride, a strong chaotrope, up to 5 M in the presence of a client protein, denatured lysozyme.

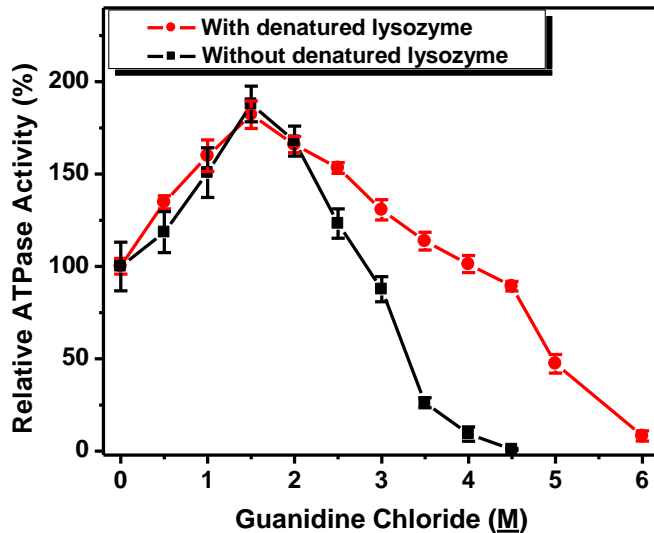


Fig 1. Binding of denatured lysozyme stimulates ATPase activity of Pfu CPN and stabilizes the complex at high concentrations (up to 5M) of guanidine HCl while ATPase activity reveals that the complex is still intact and active.

Chaperones are protein complexes that facilitate protein folding in both eukaryotes and prokaryotes. From a study of the C-terminal domains of chaperonins from hyperthermophiles, mesophiles and psychrophiles we identified a motif of charged residues, specifically in the hyperthermophiles with multiple, adjacent glu and lys residues. The *P furiosus* C-terminal contains the motif AASKLEKEKEKEGEGKGGG with five glu/lys repeats. By mutagenizing this region to reduce the charged residues we have created a matched set of chaperone complexes with a range of stability and optimal activity to operate efficiently between 30 and 103°C (Luo and Robb, 2010).

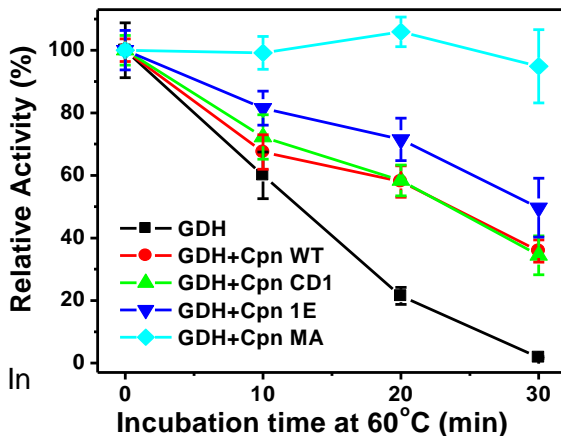


Fig. 2 Effect of site directed mutagenesis in enhancing low temperature chaperone activity of a hyperthermophilic HSP60. GDH (black squares) Decline in activity of unprotected bovine GDH. Cpn WT, protection by the wild type Cpn. Cpn CD1, complete deletion of C-terminal domain. Cpn 1E, removal of all except a single Glu (salt bridge forming) residue from the C-terminal domain. Cpn MA, mutation of all Glu residues to Ala in the C terminal domain.

protein recognition of the Cpn 60, we have devised a method for gene replacement in a genetically tractable hyperthermophile, *Thermococcus* Strain NA1. The strain has been thoroughly characterized and has novel metabolic pathways, being able to oxidize formate anaerobically with the copious production of H₂ (Kim et al, 2010). We have deleted the Cpn60 beta gene from *Thermococcus* NA1 and replaced it with a functional copy of the Pf Cpn60 without degradation of function of the *Thermococcus* NA1 growth and fermentation physiology for formate and carbon monoxide.

In Fig. 3 below, actual gene replacement and knockouts of the chaperonin HSP60 loci in *Thermococcus* Strain NA1 are depicted.

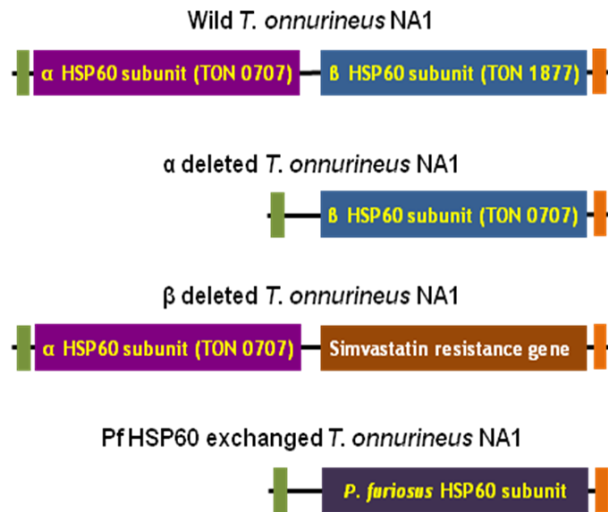


Fig 3. Schematic for cloning the thermosome genes in *Thermococcus onnurineus* NA1 using reciprocal recombination. Above, general scheme for integration of a selection cassette into the *Thermococcus* NA1 genome. provides a mechanism for genomic modification. Integration of a selectable marker cassette (gene providing positive selection, gray; promoter, bent arrow) into the genome of a recipient strain.

The resultant genome of the transformant results from two homologous recombination events between flanking regions contained in both the donor DNA and targeted genomic locus. Our current findings indicate that the Alpha subunit is adapted to the low temperature range of growth (60-75C) whereas the Beta subunit has a C-terminus very similar to the *Pyrococcus furiosus* Cpn60 and functions efficiently at 75-95C.

Our recent finding indicates that the cold-adapted mutant ATP-dependant chaperonin (Hsp60) from the hyperthermophilic archaeon *Pyrococcus furiosus* binds and fragments fibrils formed from recombinant human insulin very rapidly, with local targeted entry points.

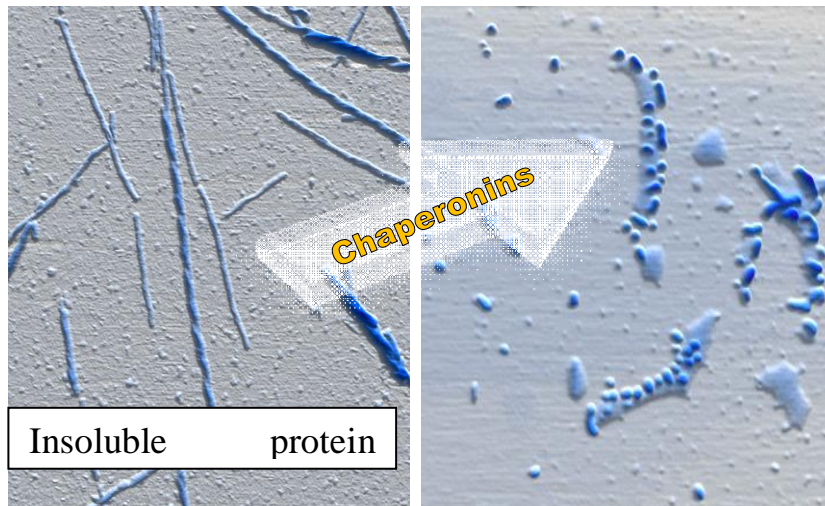


Figure 4. Salvage and solubilization activity of thermosomes during dispersion of protein fibrils. Insulin fibrils were used to compare the protofilaments in the different fibrils

were superimposed and manually aligned to find the best. In general, the protofilament shapes, sizes, and packing agree well in the different maps. Right hand panel, fibrils after Cpn60 unfolding

Individual fragments swell and the fibrillar β -sheet is quickly transformed into a mix of α -helical and unordered protein structures(2).

After further incubation, the fragments coalesced, forming large amorphous aggregates with polydisperse topologies. The modified fibrils displayed greatly enhanced cytotoxicity compared with untreated fibrils. CD and Deep UV Raman spectroscopy of the untreated and treated amyloid preparations appear in Fig. 4(1, 2).

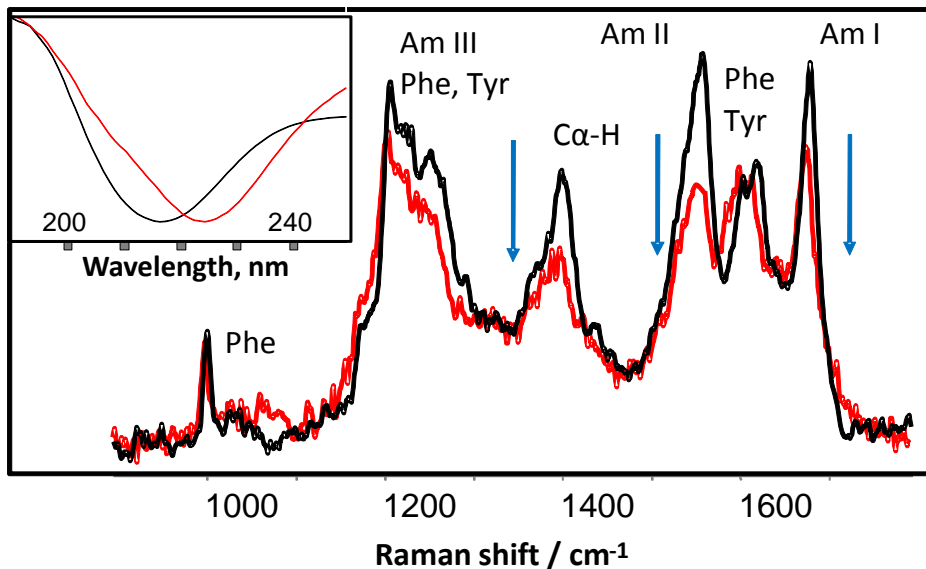


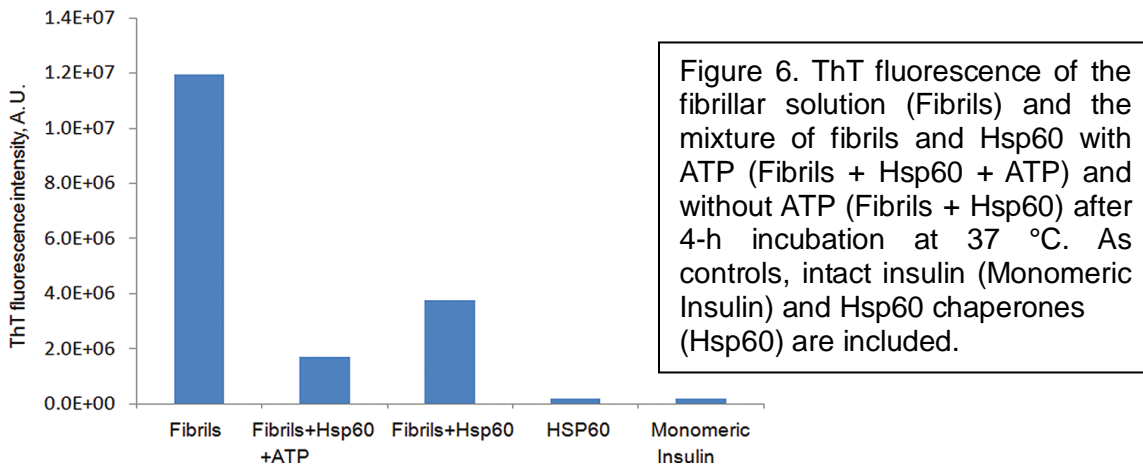
Figure 5. Deep UV resonance Raman fingerprints of protein secondary structural elements of fibrillar proteins during dispersion. Far UV CD spectra (inset) of insulin fibrils before (blue) and after treatment with chaperonin at 37°C. Deep UV Raman (DUVRR) spectra of insulin fibrils (black) and insulin fibrils treated by chaperonin (red). (from(1))

The restoration of helical content to the predominantly cross-beta structure of the

amyloid preparation is shown by the shift in the CD spectrum and in more detail in the DUVRR spectrum. The application of DUVRR spectroscopy confirmed the decrease in insulin fibrillar β -sheet content as a result of chaperonin activity (Fig. 5). The protein DUVRR spectrum is dominated by amide bands, which characterize the polypeptide backbone conformation, and aromatic amino acid bands, which report on their local environment. The spectrum of insulin fibrils shows sharp and intense Amide I and II bands as well as a strong $C\alpha$ -H band that is indicative of an extended β -sheet conformation. Both Amide I and II band intensities decreased after fibrils were exposed to chaperonins indicating the dispersion of β -sheet.(3) In addition, $C\alpha$ -H band intensity decreased indicating the formation of α -helix.

HSP6060 causes rapid β -sheet degradation with and without ATP

Insulin fibrils were selected for this study and prepared as described previously (4, 5). Insulin is a very well-studied peptide hormone that has 51 amino acids organized into two polypeptide chains linked by two inter-chain and one intra-chain disulfide bonds. Upon aggregation into fibrils, insulin molecules undergo a structural change to form a β -sheet-rich conformation (6). The thioflavinT (ThT) fluorescence assay is a universal analytical tool used to detect fibrillar β -sheets. The effects of ATP on the chaperonin-mediated transformation of insulin fibrils by ThT assays showed a decrease in β -sheet content in both the presence (2 mM) and absence of ATP (**Figure 6**). However, the presence of ATP (Fibril+Hsp60+ATP) resulted in significantly more ThT signal loss than that measured without ATP (Fibrils+Hsp60), indicating enhanced β -sheet degradation in the presence of ATP.



The initial chaperonin-fibril interaction in the absence of ATP

As previously shown, in the presence of ATP, Hsp60 rapidly deconstruct insulin fibrils to form swollen clumps (5). However, controls in which insulin fibrils were incubated without Hsp60 under the same experimental conditions (20 mM sodium acetate, pH 6.0, 2 mM ATP) at 37 °C exhibited no overall change in

fibrillar morphology (5). Fibrils were almost completely deconstructed in the presence of Hsp60 and ATP. We used atomic force microscopy (AFM) imaging to investigate the initial stage of the chaperonin-fibril interaction in the absence of ATP. Reaction mixture aliquots were deposited onto a mica substrate after 5 minutes of incubation (**Figure 7**).

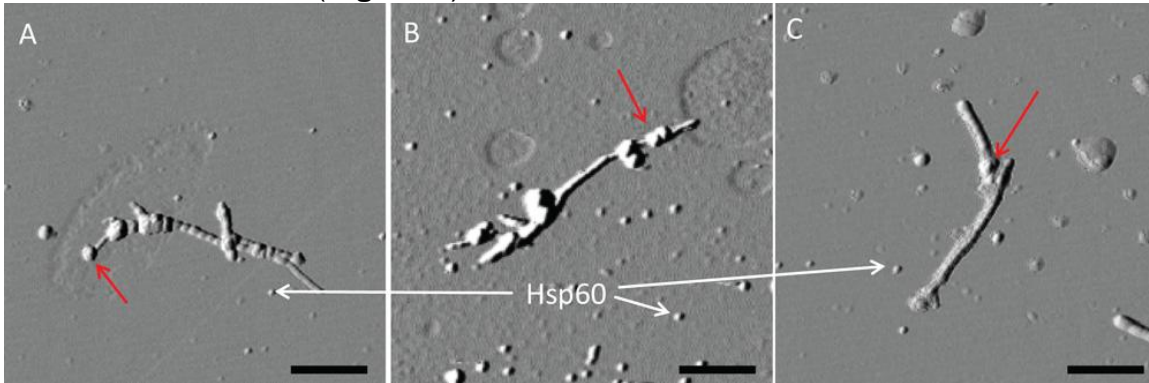


Figure 7. Insulin fibrils covered with chaperonins on their surfaces (A–C). Hsp60 were mixed with insulin fibrils without ATP for 5 min. The reaction was terminated by depositing the solution onto the mica surface with quick drying. The scale bar is 500 nm.

Morphological changes of insulin fibrils as a result of fibril-Hsp60 interaction

We utilized scanning electron microscopy (SEM) to characterize reaction products that are formed after four hours of fibril exposure to Hsp60 in the presence (2 mM) and absence of ATP. As previously reported, the deconstruction of insulin fibrils by Hsp60 results in the formation of amorphous aggregates (5). Typical images are shown in **Figures 8, panel a and b** (5). We found that Hsp60-fibril co-incubation with or without ATP leads to the formation of aggregates with similar morphology (**Figures 8, panel c and d**).

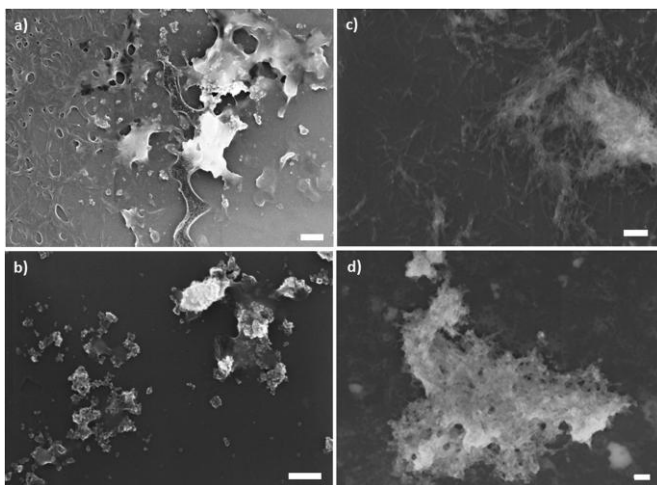


Figure 8. SEM images of the amorphous aggregates that formed as a result of insulin fibril degradation by Hsp60 with ATP (a, b) and without ATP (c, d). The scale bar is 200 nm.

We found that a substantial proportion of the original fibrils and large amorphous aggregates were evident on SEM and AFM images of the final products resulting

from chaperonin activity with no ATP present (**Figure 8, panel c**). This observation supports the hypothesis that Hsp60 is able to deconstruct insulin fibrils to form amorphous aggregates without added ATP, although the efficiency is reduced. The ThT assay indicates that some fibrillar β -sheets remain in the system after prolonged treatment with Hsp60, which could be attributed to the remaining intact fibrils seen with AFM and SEM imaging data.

The toxicity of insulin fibrils and the products of their destruction by chaperonins

The toxicity of amyloid fibrils, in general, and insulin fibrils, in particular, has been reported previously (7-9). Zacko et al. demonstrated that insulin filaments have no cellular toxicity, whereas mature fibrils are toxic to pheochromocytoma (PC 12) cells (10). An MTT assay was used to assess the toxicity of untreated insulin fibrils compared with insulin fibrils after incubation in the presence or absence of chaperonin and ATP using SHSY5Y cells. All samples exhibited dose-dependent cellular toxicity (**Figure 9, panel a**). Insulin fibrils disaggregated by Hsp60 in the presence of ATP formed highly toxic products (Fibrils+Hsp60+ATP), which exhibited enhanced cytotoxic effects compared with insulin fibrils alone, at the same dose. However, in the absence of ATP (Fibrils+Hsp60), chaperone's activity did not result in the formation of toxic products because their toxicity (Fibril+Hsp60) was almost identical to that of insulin fibrils (Fibrils).

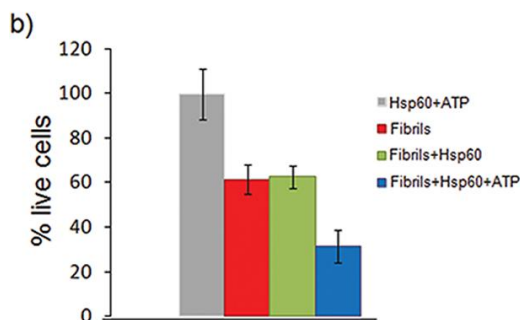
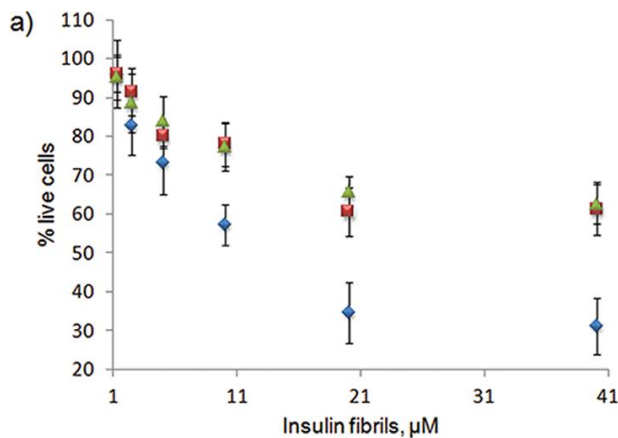


Figure 9. Insulin fibrils exhibited a dose-dependent cellular toxicity when treated with chaperonin in the presence (Fibrils + Hsp60 + ATP) and absence (Fibril + Hsp60) of ATP (a). As a control, the cellular toxicity of insulin fibrils was examined (Fibrils). ATP increased the toxicity of the insulin plus fibril and Hsp60 interaction product. Amorphous insulin aggregates (Fibril + Hsp60) resulting from Hsp60 treatment exhibited the same toxicity as the initial fibrils (Fibrils). (b) The cell toxicity (% live cells) of Fibrils (red bar), Fibrils + Hsp60 (green bar), and Fibrils + Hsp60 + ATP (blue bar) at 40 μM . Independently, Hsp60 and ATP are nontoxic to SH-SY5Y cells (gray bar).

As evident from this study, Hsp60 destroys fibril architecture and forms amorphous aggregates in the presence and absence of ATP. However, the addition of ATP significantly increases the toxicity of the fibril-Hsp60 reaction product (**Figure 9, panel a**), confirming that Hsp60 activity is activated in the presence of ATP.

Control experiments were done to determine whether cellular toxicity was associated with the presence of chaperonins rather than fibrils and their deconstruction products. Toxicity was determined in the presence of ATP and chaperonin alone (with no fibrils) (**Figure 9, panel b**). Untreated insulin fibrils (40 μ M), under the same conditions, caused significant apoptosis (60 \pm 10%). The toxicity of fibrils and Hsp60 (at the same concentration, 40 μ M) was almost identical to the toxicity of insulin fibrils alone (**Figure 9, panel b**; green and red bars, respectively). However, in the presence of ATP, Hsp60 formed highly toxic species from insulin fibrils. We found that the Fibrils+Hsp60+ATP solution exhibited almost twice the cell toxicity (**Figure 9, panel b**; blue bar) of the Fibril reaction mix and the Fibril+Hsp60 solution.

1. D. Kurouski, H. Luo, V. Sereda, F. T. Robb, I. K. Lednev, Rapid degradation kinetics of amyloid fibrils under mild conditions by an archaeal chaperonin. *Biochem Biophys Res Commun* **422**, 97 (May 25, 2012).
2. D. Kurouski, H. Luo, V. Sereda, F. T. Robb, I. K. Lednev, Deconstruction of Stable Cross-Beta Fibrillar Structures into Toxic and Nontoxic Products Using a Mutated Archaeal Chaperonin. *ACS Chem Biol*, (Aug 1, 2013).
3. V. A. Shashilov, V. Sikirzhytski, L. A. Popova, I. K. Lednev, Quantitative methods for structural characterization of proteins based on deep UV resonance Raman spectroscopy. *Methods (San Diego, Calif)* **52**, 23 (Sep).
4. D. Kurouski, R. A. Lombardi, R. K. Dukor, I. K. Lednev, L. A. Nafie, Direct observation and pH control of reversed supramolecular chirality in insulin fibrils by vibrational circular dichroism. *Chemical communications (Cambridge, England)* **46**, 7154 (Sep 1, 2010).
5. D. Kurouski, H. Luo, V. Sereda, F. T. Robb, I. K. Lednev, Rapid degradation kinetics of amyloid fibrils under mild conditions by an archaeal chaperonin. *Biochemical Biophysical Research Communications* **422**, 97 (2012).
6. D. Kurouski *et al.*, Disulfide Bridges Remain Intact While Native Insulin Converts into Amyloid Fibrils. *PLoS One* **7**, e36989 (2012).
7. V. Novitskaya, O. V. Bocharova, I. Bronstein, I. V. Baskakov, Amyloid fibrils of mammalian prion protein are highly toxic to cultured cells and primary neurons. *J Biol Chem* **281**, 13828 (May 12, 2006).
8. M. F. Mossuto *et al.*, Disulfide bonds reduce the toxicity of the amyloid fibrils formed by an extracellular protein. *Angewandte Chemie (International ed)* **50**, 7048 (Jul 25, 2011).
9. D. Patel, T. Good, A rapid method to measure beta-amyloid induced neurotoxicity in vitro. *Journal of neuroscience methods* **161**, 1 (Mar 30, 2007).
10. T. Zako, M. Sakono, N. Hashimoto, M. Ihara, M. Maeda, Bovine insulin filaments induced by reducing disulfide bonds show a different morphology,

secondary structure, and cell toxicity from intact insulin amyloid fibrils.
Biophysical journal **96**, 3331 (Apr 22, 2009).